# Low-dimensional dynamical model for the diversity of pressure patterns used in canary song

Leandro M. Alonso,[1] Jorge A. Alliende,[1] F. Goller,[2] and Gabriel B. Mindlin[1]
[1]*Departamento de Física, FCEN, Universidad de Buenos Aires, Ciudad Universitaria, Pab. I (1428) Buenos Aires, Argentina*
[2]*Department of Biology, University of UtahSalt Lake City, UT 84112 USA*
(Received 6 February 2009; revised manuscript received 23 March 2009; published 30 April 2009)

During song production, oscine birds produce large air sac pressure pulses. During those pulses, energy is transferred to labia located at the juncture between the bronchii and the trachea, inducing the high frequency labial oscillations which are responsible for airflow modulations, i.e., the uttered sound. In order to generate diverse syllables, canaries (*Serinus canaria*) use a set of air sac pressure patterns with characteristic shapes. In this work we show that these different shapes can be approximated by the subharmonic solutions of a forced normal form. This simple model is built from identifying dynamical elements which allow to reproduce the shape of the pressure pattern corresponding to one syllable type. Remarkably, integrating that simple model for other parameters allows to recover the other pressure patterns used during song. Interpreting the diversity of these physiological gestures as subharmonic solutions of a simple nonlinear system allows us to account simultaneously for their morphological features as well as for the syllabic timing and suggests a strategy for the generation of complex motor patterns.

DOI: 10.1103/PhysRevE.79.041929 PACS number(s): 87.19.−j

## I. INTRODUCTION

The development of song in songbirds is a prime biological model for understanding the interaction between nature and nurture. Just as in humans, oscine birds, parrots, and some hummingbirds require experience with a tutor to eventually develop species-typical song [1]. For these reasons, in the last years many disciplines have converged in their efforts to unveil the mechanisms behind vocal learning in these birds. A complex neural architecture has been described to be responsible for generating the patterns of activity, which are transduced into specific physiological commands controlling the vocal peripheral system [2].

Physics has participated in this collective effort by integrating a large body of experimental work with the expected basic mechanical processes involved in birdsong production. Through this integrative approach a more complete picture starts to emerge about the respective roles and synergies of different muscles used by a singing bird [3]. The physical models have therefore helped put in perspective the role of different muscles in the generation of specific rhythmic and melodic features of the song. The program has been particularly successful in understanding production of tonal song in some oscines, as for example cardinals and canaries [4,5].

For these cases, experimental work and theoretical analysis have highlighted the physiological role played by different motor patterns. Activity of ventral syringeal muscles, for example, is fundamental in the frequency control of the syllables [5–7]. Dorsal syringeal muscles, on the other hand, play a major role in closing the syringeal valve and thus regulate airflow. But the process of vocalizing itself does not start until the bird generates respiratory pressure sufficiently high for airflow to turn on labial oscillations (see Fig. 1), in a process similar to the way in which humans vocalize voiced sounds. In this work we focus on this last motor pattern: the one responsible for the air sac pressure pulses.

Canary song is hierarchically structured: brief, stereotyped tonal syllables are repeated many times, to form "phrases." These are combined in a variable order to form songs [8]. Typically, different phrases consist of syllables repeated at a characteristic syllabic rate. In terms of the air sac pressure, different syllabic types are uttered with different pressure patterns [9]. For example, the fastest syllable repetition rates (30–60 Hz) in canary song are generated with a sustained expiratory pressure pulse with small oscillations. Lower syllable repetition rates (<30 Hz) are typically generated with short expiratory air sac pressure pulses which alternate with short inspirations (mini-breaths).

In this work we test the hypothesis that a unique dynamical mechanism underlies the diversity of pressure gestures of different syllables. We write a low-dimensional system of

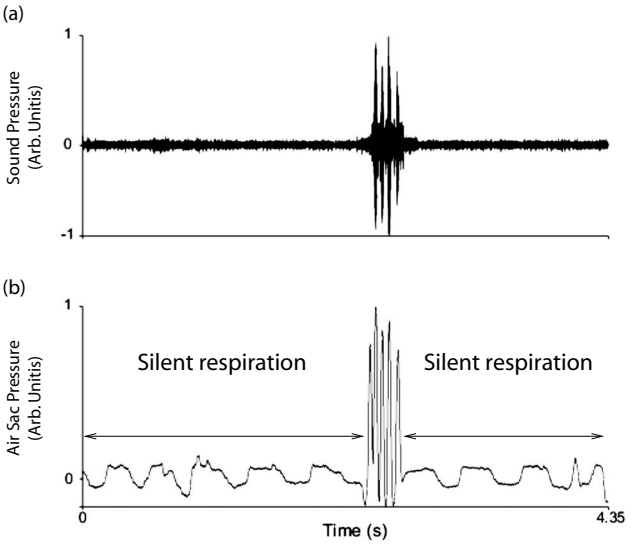


FIG. 1. Sound (a) and air sac pressure (b) for a canary uttering four calls. Notice that during silent respiration, the air sac pressure oscillates around zero. During the vocalizations, the air sac pressure is increased. Each uttered sound is associated with a large expiratory pulse. The amplitude of these pulses is several times larger than the expiratory fluctuations during silent respiration.

 

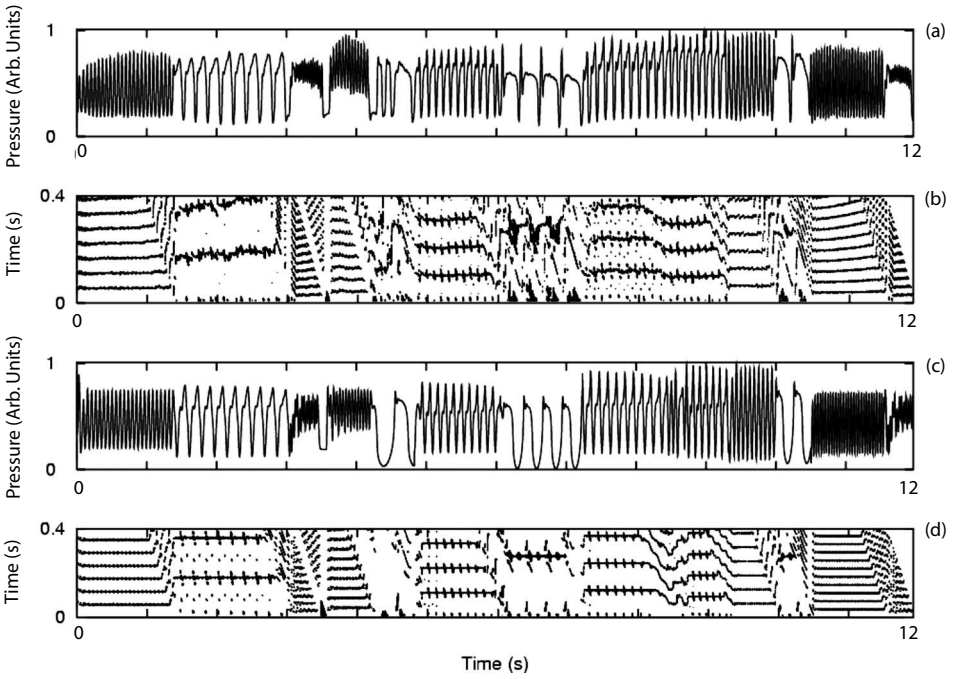


FIG. 2. The experimental record of the air sac pressure recorded in a canary (bird number 1) during a complete song (a). The close return plot corresponding to the same time series data (b). The horizontal lines denote the existence of recurrencies. A synthetic air sac pressure obtained by integrating the equations of the model described in the text. The values of $(A,\theta,\omega)$ were changed so that the different pressure patterns pressure could be well approximated, and kept constant during the time in which a syllable was being repeated (c). The close return plot of the displayed synthetic solution (d).

equations whose different solutions are similar to the experimental time traces. We test the hypothesis fitting the parameters of a very simple dynamical system (a forced normal form), and showing that the synthetic solutions can fit both the shapes of the pressure patterns, as well as the relative timing of the modeled syllables.

This work is organized as follows. The data are presented in Sec. II, while the mathematical model being proposed is written in Sec. III. This model was written so that the pressure pattern of one particular syllable could be reproduced. Remarkably, changing the forcing parameters allows us to recover the shapes of the pressure patterns associated with the other syllables. Moreover, when the relative timing between syllables is reproduced, so are the different pressure patterns. This material is presented in Sec. IV. Section V presents a discussion and our conclusions.

## II. DATA

Three adult male canaries (*Serinus canaria*) were used in this study. They were given seed and water *ad libitum*, housed in individual cages ($30\times25\times30$ cm), and maintained in a 14:10 h light:dark cycle. They were bought from different local breeders and therefore had different learning experiences. In front of each cage a microphone was placed in order to record the produced song with a multichannel sound card (MAYA 1010, 44.1 kHz sample rate) directly onto a computer. Simultaneous recordings of sound and subsyringeal air sac pressure were made. The time series corresponding to air sac pressure was registered by the insertion of a cannula (venisystemsAbbocath-T) through the abdominal wall just posterior to the last rib, so that it extended a few millimeters into a thoracic air sac. The free end of the cannula was connected to a miniature piezoresistive pressure transducer (Fujikura model FPM-02PG), which was mounted on the bird's back [7]. The signal was amplified and modulated in order to record it onto a computer with the same sound card used to record sound. The insertion of the cannula was made with the bird anesthetized with intramuscular injection of ketamine/xilazyne. Birds usually started singing 1–2 days after the surgery. In this way, we generated time traces corresponding to pressure in arbitrary units sampled at 44.1 kHz. Each data file included at least a complete song, with each song lasting approximately 10 s [10,11].

Figure 2 displays a pressure record during a typical song (a). The existence of recurrencies is easy to recognize from a first inspection of the data, where the term recurrencies denotes the existence of a pattern that almost repeats itself. In the field of nonlinear dynamics, there is a particularly appropriate technique to investigate temporal recurrencies. It is called the close return plot, which is a graphical representation of the recurrencies present in the signal. In order to build these plots, the time series under analysis is stored in a vector $v[i]$, for $i=1,\ldots,n$, with $n$ the number of samples. Then, the distance $d(i,p)$ between the values stored at $v[i]$ and $v[i+p]$ is computed as $d(i,p)=abs(v[i]-v[i+p])$, for pairs of integer values $(i,p)$. Whenever the distance is smaller than a threshold value $\epsilon$, a point is displayed at coordinates $(i,p)$. In this way, an almost periodic signal will be reflected in the close return plot as a straight line, with a length proportional to the time that the sound signal remains almost periodic.

In Fig. 2(a) we display the air sac pressure of one of the individuals studied during singing. In Fig. 2(b) we display the close return plot corresponding to the time series in Fig. 2(a). As it could be expected from a simple inspection to the time series data, there are time intervals in which the pressure behaves almost periodically. Less obvious is that the repetition time of the different syllables does not seem to be completely arbitrary. For example, the repetition time during the second syllable displayed in Fig. 2(a) is three times larger than that of the first syllable.

Just as there is stereotopy in the rhythms across different individuals, the pressure patterns time series corresponding

to different syllables display features which are found across different individuals. For example, in the songs of all the individuals which we studied these patterns have been found: simple, almost harmonic oscillations, high frequency fluctuations around a dc level, oscillations presenting wiggles, and long lasting pressure pulses. Moreover, birds subjected to different learning experiences presented pressure patterns with similar shapes.

A parsimonious hypothesis is that the diversity of respiratory motor gestures emerges from an equally diverse and complex system. Alternatively, the diversity could be accounted for by the different solutions that a unique nonlinear system can present for different parameters. If the latter model is the case, the set of diverse solutions is severely constrained by the geometric mechanisms involved in its generation. Here we test this hypothesis.

### III. MODEL

In order to generate the precise pressure patterns needed to produce a song, an oscine bird uses a complex neural architecture. The "songbird motor pathway" is a set of interconnected neural nuclei (each one composed of a few thousand neurons) which are indispensable for birdsong generation. The electrical pattern of activity emerging out of this physical substrate eventually is transduced into activity of the appropriate muscles controlling the respiratory gestures. Attempts have been made to implement "comprehensive" [12] models for these neural systems [13]. Yet, the large number of neural units involved and the complexity of its connectivity make experimental exploration difficult. In order to test the hypothesis that despite the large amount of degrees of freedom in the problem, the measured patterns are the solutions of a low-dimensional dynamical system, we followed a different approach. We built a simple dynamical system whose solutions can reproduce the measured patterns. This dynamical system is, in a sense, minimal: it is the forced normal form of a linear singularity.

In order to build our model, we started inspecting the pressure pattern displayed in Fig. 3(a). This pattern is found in every song, of every bird analyzed. It consists of a long expiratory pulse, associated with the syllables uttered at the lowest syllabic rate. The pressure starts at the average value of the nonsinging regime, rapidly increases until it reaches a large value, staying close to it for a certain amount of time (typically of 200 ms), to finally return to the initial pressure value.

We will call the initial value of the pressure the "off" state, the high value approached during the vocalization as the "on" state, and conjecture that the searched dynamical system has both states as different fixed point attractors for different parameters. In other words, in the dynamical scenario that we propose, the system was initially in a stable equilibrium of the searched dynamical system (the off state). At a given time [represented by (1) in Fig. 3(b)], the parameters of the model were changed in such a way that the off state ceased to exist, and the system evolved to a different attractor [the on state, represented by 2 in Fig. 3(b)]. After a while, we conjecture that the parameters of the model were

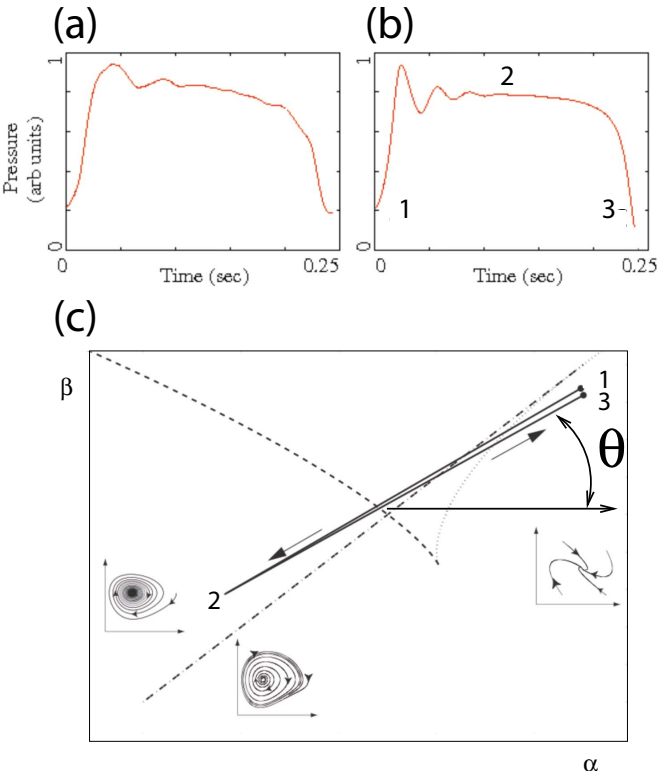


FIG. 3. (Color online) The parameter space diagram of the autonomous model proposed in the text (c). The two curves converging at a cusp are saddle node curves. Bounded by these curves two attractors exist, separated by a saddle fixed point. The third curve in the figure is a Hopf bifurcation curve. The arrows indicate a path followed in the parameter space in order to generate the experimental record displayed in (a). Integrating the model with the time-dependent parameters represented by the arrows in part (c), we synthesize the time series shown in (b).

changed back to their original values; the on state ceases to exist, and the system returns to the original fixed point representing the off state. One way to write a dynamical system capable of displaying this behavior is to build it in such a way that it presents a cusp bifurcation [see Fig. 3(c)]. In this codimension two bifurcation, two saddle node curves collide at a point in parameter space. For some region of the parameter space, three points exist: two attractors and a saddle. Outside this region, only one attractor is present. Assuming that our dynamical system is close to a cusp, and initially at the parameters where only one fixed point exists (the off state), it can jump to a different attractor as the parameters are moved across the three fixed point region of the parameter space. The on state is born together with a saddle, which collides with the off state when the parameters are further moved away from the three fixed point region of the parameter space. Yet, a one-dimensional dynamical system presenting a cusp bifurcation would not be suitable for reproducing the observed dynamics. Notice that when the pressure increases its value toward what we call the on state, it displays a couple of small amplitude, damped oscillations. We conjecture then that the searched dynamical system should be at least two dimensional, and moreover, the on state should be an attractor somewhat close to a Hopf bifurcation. In a two-

dimensional parameter space, the Hopf bifurcation line and the saddle node curves should meet. Therefore, our starting parameters are chosen as the ones at which one of the saddle node curves mentioned above, and the Hopf curve meet. We build the normal form for this linear singularity as

$$\dot{x} = y,$$

$$\dot{y} = x^2 - xy - x^3 - x^2 y, \tag{1}$$

which is the normal form for the Takens-Bogdanov bifurcation. We included third-order terms in our normal form in order to allow three fixed points to exist. The signs in the normal form guarantee the existence of super critical Hopf bifurcations, and the existence of two stable fixed points in its unfolding. We claim that the different states displayed by our system are reached as the systems parameters are varied. Therefore, unfolding this bifurcation with time-dependent parameters leads to

$$\dot{x} = y,$$

$$\dot{y} = \alpha(t) + \beta(t)x + x^2 - xy - x^3 - x^2 y. \tag{2}$$

In Fig. 3(b), we display the numerical integration of our dynamical model as the parameters are moved along the trajectory displayed in Fig. 3(c). The system is originally in a region of the parameter space where a fixed point attractor exists, then the parameters are moved toward a region where a different fixed point solution with imaginary eigenvalues and real part smaller than zero exists, and finally, the parameters are returned to their initial values. The observed pressure in our model is represented by $p(t)=2-x(t)$ where $x(t)$ is a solution of Eq. (2).

In order to generate the different pressure patterns, we drive the system using a particular form of $\alpha(t)$ and $\beta(t)$, namely,

$$\dot{x} = y,$$

$$\dot{y} = \alpha_0 + A\cos(\theta)\cos(\omega t) + [\beta_0 + A\sin(\theta)\cos(\omega t)]x + x^2 - xy - x^3 - x^2 y. \tag{3}$$

We fixed $\alpha_0=1$, $\beta_0=3$ and we applied a rescaling of time $t=35\tau$. These parameters are the same for all birds analyzed in this work. Parameter $A$ represents the amplitude of the forcing, $\omega$ is the frequency, and $\theta$ is the direction of the forcing in the $(\alpha,\beta)$ plane as shown in Fig. 3(c).

If we were to synthesize pressure patterns where this basic gesture is repeated, as it is usually the case during song, we can repeat this basic driving. Yet, the model is nonlinear, and therefore the range of frequencies for which the system will display this simple behavior is bounded. For higher forcing frequencies, the system can display subharmonic solutions.

We will test the hypothesis that all the pressure patterns found in the generation of canary song can be fitted with this simple model, changing the forcing parameters. In this way, the distinctive shapes of the pressure patterns used to generate different syllables would not be arbitrary: syllables of a given syllabic rate should present particular shapes.

## IV. FITTING PARAMETERS

A typical result is illustrated in Fig. 2, in which we show both the experimentally recorded time series data of the air sac pressure (top panels), and the synthetic time series obtained by numerical integration of the forced normal form presented in Sec. III. In order to generate the synthetic time series emulating the behavior of a complete song, a set of numerical simulations of the forced normal form [Eq. (3)] was carried out. We used different sets of parameters in order to synthesize the different pressure pattern types. In this section we describe the procedure followed in order to select these sets of parameters.

The top panel of Fig. 2(a) shows the experimental pressure pattern recorded for one experimental subject. Figure 2(b) shows the close return plot of the time series above [14,15]. The nearly straight horizontal lines suggest recurrence in certain segments of the song. For a given segment of the time series presenting recurrent behavior, the height of the lowest horizontal line (vertical axis) appearing in its close return plot indicates the time of the recurrence (i.e., its approximate period). Suggestively, the different heights of the horizontal lines corresponding to different segments displaying recurrency are not completely arbitrary. For example, the heights of the two first segments are in a 1:3 ratio. This behavior would be consistent with the hypothesis that these recurrences are different subharmonic responses to a periodic driving with similar frequencies.

Each experimental time series was then divided into smaller segments for which the close returns plot displayed nearly horizontal lines. Each one of these segments corresponds to different pressure pattern types. In this way, each segment of the recorded pressure pattern is almost periodic and they were fitted using different periodic solutions of the model.

The fitted parameters were those corresponding to the forcing terms, and a scaling factor of the synthetic pressure pattern. The forcing is determined by its amplitude $A$, its frequency $\omega$, and its direction $\theta$ in the $(\alpha,\beta)$ plane [see Fig. 3(c)].

As was mentioned in Sec. III, the vector field used to model our experimental results was inspired by one specific orbit type. We explored numerically the different solutions that arise as the forcing parameters were swept over a wide range. A systematic study of the solutions showed that many morphological features found in the experimental orbits could be recovered. Over open sets of the parameter space we could find solutions which looked like harmonic oscillations, small oscillations mounted on a dc level, as well as orbits presenting small wiggles. This is a remarkable finding. Nonlinear systems can be classified according to the topological organization of its period orbits [16]. In other words, not every dynamical system can present a range of periodic solutions that can reproduce a set of arbitrary shapes. The fact that fitting one particular solution allows us to eventually find (for the adequately chosen parameters) the rest of the experimental patterns builds confidence in the simple proposed model. Moreover, it leads us to implement an algorithmic procedure for fitting the parameters of the forcing. In order to fit a particular segment of the time trace which pre-

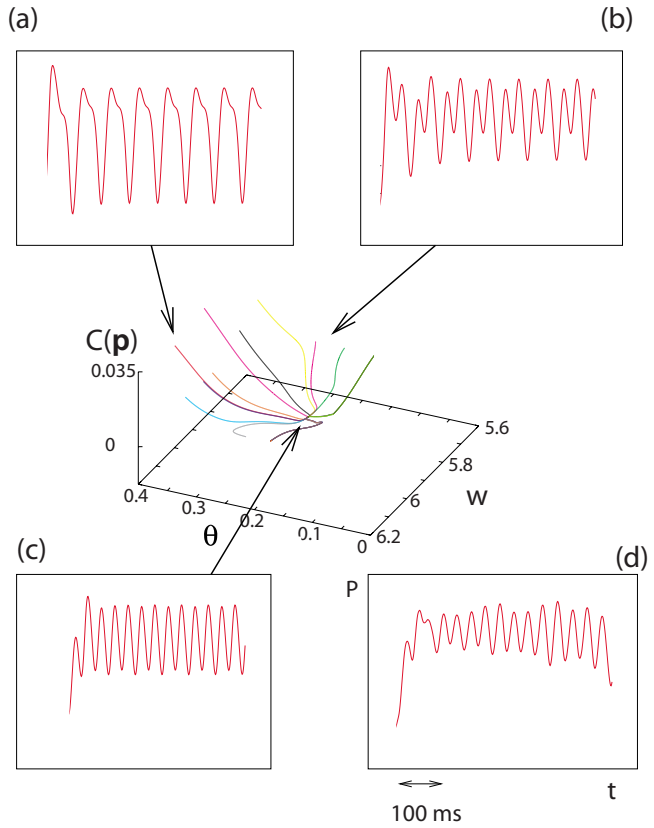


FIG. 4. (Color online) An illustration of the steepest descend method applied to fit the model. With initial parameters giving rise to the synthetic time traces displayed in the panels (a) and (b), we start a search for the parameters minimizing $C$, the cost function that measures, for each set of parameters, the difference between a synthetic solutions integrated with those parameters, and the experimental data. Panel (c) illustrates the solution obtained by the optimal parameters, which approximates the experimental record displayed in panel (d).

sented a clear recurrent behavior, the first step was to choose a set of parameters for which the vector field presented solutions with similar morphological features. Then, an algorithm was run in order to obtain the parameters that would minimize a function measuring the difference between the synthetic signal and the data.

We define a cost function of the system $C(p)$ as

$$C(\mathbf{p}) = \frac{1}{\mathbf{T_{exp}}} \int_0^{\mathbf{T_{exp}}} [\mathbf{X(p,t)} - \mathbf{E(t)}]^2 \mathbf{dt}, \tag{4}$$

where $E(t)$ stands for the experimental time trace, $\mathbf{p} = (\mathbf{A}, \theta, \omega)$ (the parameters of the forcing), $T_{\text{exp}}$ is the duration in seconds of the pressure pattern being analyzed, and $X(p,t)$ is a solution of the system 3 integrated with parameters $\mathbf{p}$ and fixed initial conditions. $T_{\text{exp}}$ ranges from 1 to 4 sec depending on the pattern being analyzed. Our aim was to find local minima of this function to determine the set of parameters that best fits each pattern. All the model generated patterns shown in this work correspond to local minima of this function.

Since the hypothesis to be tested is whether subharmonicity is responsible for the diversity of measured patterns, we started the algorithmic procedure by choosing a region in the parameter space such that subharmonic solutions displaying shapes similar to the observed ones were present. Our simulations showed that the parameter $\theta$ was critical: some subharmonic solutions would not be present outside a small range of this parameter. Once $\theta$ takes a value such that the desired subharmonic behavior was found, we implemented a gradient descend method to find local minima of the cost function. Once a minimum was found, we checked that the synthetic pattern would reproduce the basic morphological features described in the previous section.

In all our searches, the initial conditions corresponded to an "off" state. No transient was eliminated in our numerical simulation. Therefore, fitting the right recurrent experimental patterns required not only being able to find a periodic solution with the right shape, but also finding it stable enough so that an off state would rapidly converge to the desired pattern. This requirement allows us to reproduce synthetically long songs consisting of several different pressure patterns, as in Fig. 2(c) with a unique initial condition. For simulating a long song, we only had to change at the right times the features of the forcing, without resetting the initial conditions. It is important to realize that some patterns can be

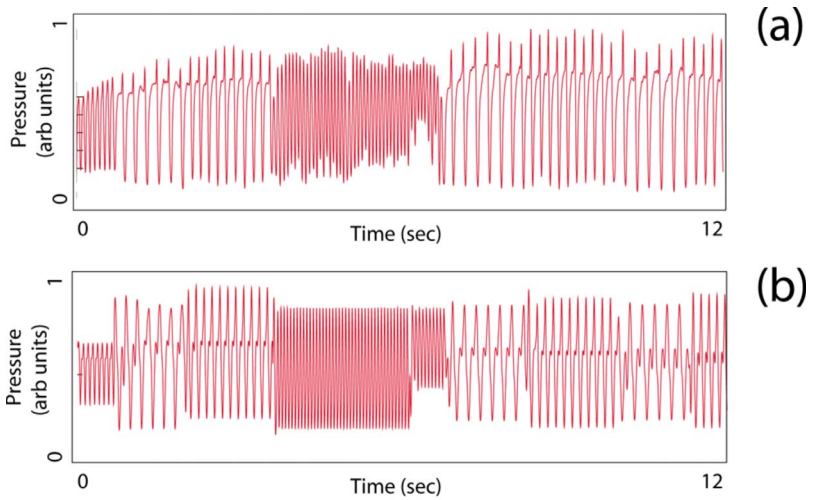


FIG. 5. (Color online) The experimental record (a) and synthetic solution (b) for bird number 2. The parameters were changed in this numerical experiment at each time there was a change in the experimental pressure pattern type.

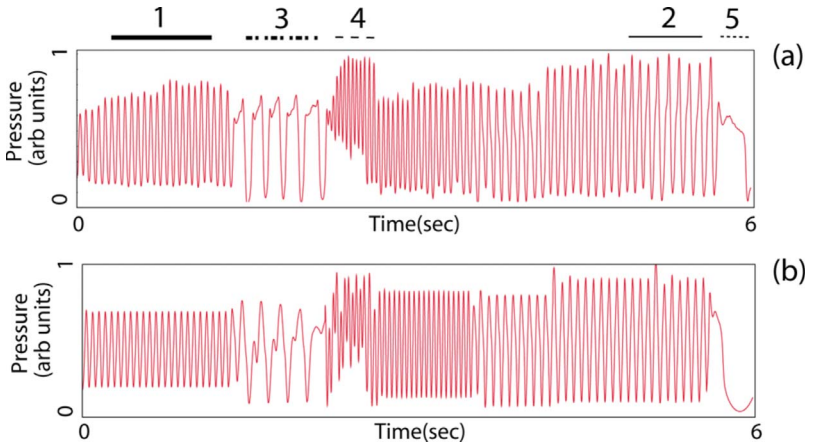


FIG. 6. (Color online) The experimental record (a) and synthetic solution (b) for bird number 3. The parameters were changed in this numerical experiment at each time there was a change in the experimental pressure pattern type. The numbers in the upper panel (a) indicate the type of pattern. Pattern type 5 is treated separately, since it is the one used to build the model

fitted with different solutions. For example, a given pattern can be fitted as a period 3 solution with a forcing frequency $\omega_f = \omega/3$, or as a period 1 solution with a forcing frequency $\omega_f = \omega$. In those ambiguous cases, the solution minimizing the cost function was chosen.

Once a suitable starting zone in parameter space was identified, we computed

$$G_i = C(p + dp_i) - C(p), i = 1,2,3, \tag{5}$$

where $dp_i$ was chosen as $dp_i = 0.000001$. This quantity can be thought of as the gradient of the cost function. We moved in parameter space in such a way that in each step, the parameters would lead to lower values of the cost function. This was achieved by changing $\mathbf{p}$ in the direction of the gradient by an amount $k \times G_i$ with $k = 0.001$. The algorithm ends when $G_i < \epsilon$ with $\epsilon = 0.000001$ and thus guarantees that a $dp_i$ perturbation of the solution $X(p,t)$ yields higher values of the cost function. In Fig. 4 we display several trajectories in parameter space during our fitting procedure. For a diversity of initial parameters, we show the evolution of the cost function. A local minima is found where the synthesized pressure gesture resembles the experimental one [see panels (c) and (d) in Fig. 4]. In Figs. 5 and 6 experimental and synthesized pressure gestures for two different birds are presented. Patterns were synthesized as describe before, without changing the initial conditions.

In Table I we show the parameters found when fitting three experimental recordings corresponding to complete songs of three different birds. In Fig. 7 we display the fitted values in the $(A, \theta, \omega)$ space. There is a clustering of the parameters when grouped by pattern type. The lines in the figure sketch the boundaries of the contiguous regions of the parameter space where the fitted equations display different subharmonic solutions. These regions are the three-dimensional version of what in the literature of forced oscillators are known as Arnold tongues. Their complex structure does not allow to recognize the clustering of the point types if only one fitted parameter is inspected at the time. In the figure, the pattern types 1 and 4 are drawn together since both correspond to period 1 solutions of our forced dynamical system. Remarkably, the different birds, which were not contemporary in the laboratory, and were bought as adults from different breeders (therefore, they were exposed to different tutors), present pressure patterns which can be fitted with the same dynamical system, with well clustered parameters.

## V. DISCUSSION AND CONCLUSIONS

A low-dimensional system of coupled differential equations was proposed to model the pressure patterns in the air

TABLE I. Parameters found when fitting three experimental recordings corresponding to complete songs of three different birds. The reference for pattern types is depicted in Fig. 6. The parameters are sorted by ascending $\theta$.

| Bird number | $A$ | $\theta$ | $\omega$ | Pattern type |
|---|---|---|---|---|
| 1 | 55 | 0.02 | 4.89 | 1 |
| 1 | 30 | 0.03 | 3.08 | 1 |
| 2 | 35 | 0.09 | 3.1 | 1 |
| 3 | 35 | 0.09 | 4.55 | 1 |
| 3 | 30 | 0.1 | 3.51 | 1 |
| 3 | 45 | 0.15 | 5.72 | 4 |
| 1 | 42.98 | 0.16 | 5.61 | 4 |
| 1 | 43.03 | 0.35 | 4.08 | 4 |
| 3 | 40 | 0.5 | 5.52 | 2 |
| 2 | 24.88 | 0.5 | 2.87 | 4 |
| 2 | 25.9 | 0.68 | 2.13 | 1 |
| 3 | 14.97 | 0.72 | 3.46 | 3 |
| 2 | 10.85 | 0.78 | 2.69 | 3 |
| 1 | 12.4 | 0.79 | 3 | 3 |
| 3 | 36 | 0.8 | 5.69 | 2 |
| 3 | 36 | 0.81 | 5.69 | 2 |
| 1 | 36.05 | 0.88 | 5.67 | 2 |
| 1 | 23.45 | 0.92 | 4.83 | 3 |
| 1 | 30.4 | 0.93 | 5.66 | 3 |
| 2 | 9.55 | 0.99 | 2.44 | 3 |
| 2 | 9.98 | 1 | 2.55 | 3 |
| 1 | 19.96 | 1.02 | 4.4 | 3 |
| 2 | 15.95 | 1.07 | 3.8 | 3 |
| 2 | 16.1 | 1.07 | 3.81 | 3 |
| 2 | 15.4 | 1.1 | 3.69 | 3 |

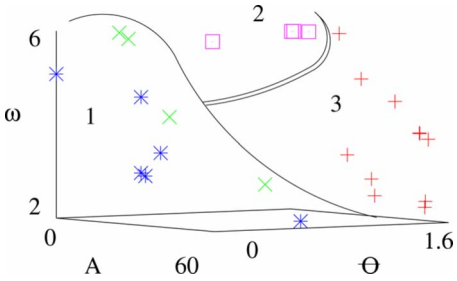


FIG. 7. (Color online) The fitted parameters listed in Table I, in the $(A, \theta, \omega)$ space. The different point types are associated with different pressure pattern types. They are found within regions of the parameter space where the model presents different subharmonic solutions. The continuous lines sketch the boundaries of those regions. The pattern types 1 and 4 are drawn in the same regions since both correspond to period 1 solutions of our forced dynamical system.

sacs of *Serinus canaria* during song production. Despite the complexity exhibited by these patterns, we were able to find solutions of this model that resemble the main features. In order to propose this model, we analyzed one particular simple pattern and engineered a transition between simple dynamical states which would give rise to a time series similar to the experimental patterns. The proposed dynamical system was a normal form presenting these dynamical elements. Remarkably, when the system was numerically explored for different sets of parameters, solutions similar to the other pressure patterns were found.

The agreement was qualitative and quantitative. In fact, we implemented a simple gradient descend method to fit the parameters in our dynamical system. By doing so we checked that different birds presented patterns which could be fitted by well clustered parameters. Actually, the main reason for this clustering is that the different patterns are approximated by the model with subharmonic solutions of a nonlinear driven system. The different subharmonic solutions exist in bounded regions of the parameter space (Arnold tongues), and therefore the clustering of the different syllabic types is associated with this bounding.

Not every set of time series data can be approximated by the solutions of a unique low-dimensional dynamical system. Dynamical systems can be classified by the topological organization of its solutions [16]. In a three-dimensional nonlinear dynamical system, the linking organization between different periodic solutions, the self-linking of a unique orbit, or its knot type [15] have to satisfy a specific set of conditions. Therefore, the existence of a low-dimensional model for the different pressure patterns used in phrases by singing canaries suggests that despite the complexity of the neural architecture used to generate these physiological instructions, they have to act collectively in a way that ultimately translates into a low-dimensional instruction. It is worth pointing out that despite this reduction of dimensionality, the diversity between the shapes is surprising, and suggests a strategy for achieving diverse behavior: the use of subharmonicity of a nonlinear neural substrate.

Previous works have suggested that the pressure patterns behaved as subharmonic [17,18]. Yet, these efforts explored mathematically rate models for the activities of specific neural architectures which could be responsible for generating the instructions. Different architectures could display this behavior. In this work, we performed a systematic fitting of the diversity of pressure patterns present in all the songs of three birds, using a dynamical model. The dynamical elements that were necessary for building that system (which being a normal form, is in a sense minimal in complexity) have to be present in the mathematical implementation of any neural model proposed to account for the observed behavior.

Not every oscine bird has a song consisting of repeated syllables. Another well studied songbird, the zebra finch (*Taeniopygia guttata*) builds its song with a stereotyped sequence of syllables presenting a wide range of acoustic properties, and therefore the strategy for generating its pressure patterns seems different as the one described in this work. Yet, it is worth exploring whether other species building songs with phrases of repeated syllables could use subharmonicity in order to generate diversity with minimal nonlinear substrates.

## ACKNOWLEDGMENTS

This work was financially supported by UBA, NIH, and CONICET. All experimental procedures were approved by the Institutional Animal Care and Use Committee of the University of Utah.

[1] H. Hultsch and D. Todt, *Nature' s Music*, edited by P. Marler and H. Slabbekoorn (Elsevier, Amsterdam, 2004).
[2] E. D. Jarvis, *Nature' s Music*, edited by P. Marler and H. Slabbekoorn (Elsevier, Amsterdam, 2004).
[3] R. A. Suthers, F. Goller, and C. Pytte, Philos. Trans. R. Soc. London, Ser. B **354**, 927 (1999).
[4] T. Gardner, G. Cecchi, M. Magnasco, R. Laje, and G. B. Mindlin, Phys. Rev. Lett. **87**, 208101 (2001).
[5] G. B. Mindlin, T. J. Gardner, F. Goller, and R. Suthers, Phys. Rev. E **68**, 041908 (2003).
[6] F. Goller and R. A. Suthers, J. Neurophysiol. **76**, 287 (1996).
[7] F. Goller and R. A. Suthers, J. Neurophysiol. **75**, 867 (1996).
[8] T. Gardner, F. Naef, and F. Nottebohm, Science **308**, 1046 (2005).
[9] R. S. Hartley and R. A. Suthers, J. Comp. Physiol. [A] **165**, 15 (1989).
[10] M. A. Trevisan, J. M. Mendez, and G. B. Mindlin, Phys. Rev. E **73**, 061911 (2006).
[11] J. M. Mendez, J. A. Alliende, A. Amador, and G. B. Mindlin, Phys. Rev. E **74**, 041917 (2006).
[12] F. C. Hoppensteadt and E. M. Izhikevich, *Weakly Connected Neural Networks* (Springer-Verlag New York, Inc., Secaucus,

NJ, 1997).
[13] H. Abarbanel, L. Gibb, G. B. Mindlin, and S. Talathi, J. Neurophysiol. **92**, 96 (2004).
[14] G. B. Mindlin and R. Gilmore, Physica D **58**, 229 (1992).
[15] G. B. Mindlin, H. G. Solari, M. A. Natiello, R. Gilmore, and X. J. Hou, J. Nonlinear Sci. **1**, 147 (1991).
[16] G. B. Mindlin, X. Hou, H. Solari, R. Gilmore, and N. B. Tufillaro, Phys. Rev. Lett. **64**, 2350 (1990).
[17] M. Trevisan, G. B. Mindlin, and F. Goller, Phys. Rev. Lett. **96**, 058103 (2006).
[18] E. Arneodo, L. Alonso, J. A. Alliende, and G. B. Mindlin, Pramana, J. Phys. **70**, 1077 (2008).